Supporting Information

Facile construction of Fe, N and P co-doped carbon spheres by carbothermal strategy for adsorption and reduction of U(VI)

Zhimin Dong,[a] Zhibin Zhang,[a*] Runze Zhou,[a] Yayu Dong,[b] Yuanyuan Wei,[a] Zhijian Zheng,[a] Youqun Wang,[a] Ying Dai,[a] Xiaohong Cao,[a] Yunhai Liu[a*]

[a]*State Key Laboratory of Nuclear Resources and Environment, East China University of Technology, Nanchang, Jiangxi 330013, P.R. China*

[b]*MIIT Key Laboratory of Critical Materials Technology for New Energy Conversion and Storage School of Chemistry and Chemical Engineering, Harbin Institute of Technology, Harbin 150001, P.R. China*

***Corresponding Authors:** E-mail: Walton_liu@163.com (Y.H. Liu), zhbzhang@ecut.edu.cn (Z.B, Zhang).*

***S1* Materials**

Acrylonitrile (AN, 99.9%, Aldrich) were purified by distillation under reduced pressure to remove the stabilizer. Potassium persulfate (PPS, Sigma-Aldrich), sodium dodecylsulfate (SDS, Sigma-Aldrich) and other chemicals were all analytical grade and without further purification. 20 mL hydrochloric acid (ρ= 1.18 g□mL^{-1}), 2 mL 30% hydrogen peroxide were added into a 100 mL beaker containing of 1.1792 g U_3O_8 successively. The mixture was heat to nearly waterless and then 10 mL nitric acid (ρ= 1.42 g□mL^{-1}) was put into the beaker. The solution transferred to a 1000 mL volumetric flask was diluted to the mark line with distilled water to obtain a UO_2^{2+} stock solution (1.0 mg□mL^{-1}).

S2 Characterizations

The XRD patterns were recorded with a reflection mode (Cu Kα source, λ=1.5412 Å) in 2θ=2º-80º with a scanning rate of 1º· min^{-1}. Data of FT-IR (Fourier transform infrared spectroscopy) spectra were carried out on Nicolet-5700 FT-IR spectrophotometer with a potassium bromide pellet in the 4000 - 400 cm^{-1} region. The morphologic characterization was carried out on a field emission scanning electron microscope (FE-SEM, JEOLJSM-7001F, Japan) and TEM (JEOL-2100). Nitrogen sorption isotherms at 77 K were measured on a Micrometitics Tristar 3000 system. Before measurement, samples were pre-treated at 373 K for 12 h under nitrogen blowing. The specific surface area and the pore size distribution were calculated from the BET and BJH data. The zeta potential values were measured with a Zetasizer Nanosizer ZS instrument (Malvern Instrument Co.). X-ray photoelectron spectroscopy (XPS) measurements were conducted on a Thermo Fisher Scientific ESCALAB 250Xi spectrometer.

S3 Batch experiments of U(VI) sorption

The adsorption experiments were carried out by batch technique. Briefly, the stock dispersal of absorbent material (0.10 $g \cdot L^{-1}$) was added into U(VI) solution (0-110 $mg \cdot L^{-1}$) under vigorous stirring conditions. After shaking 5 h for attaining the adsorption equilibrium, the solid and liquid phases were separated by the centrifugation at 8000 rpm for 15 min and subsequently the U(VI) concentration of upper solution was analyzed via the arsenazo III method using a visible spectrophotometer at 650 nm [1]. The quantity of adsorbed U(VI) on adsorbent was deduced from the dissimilarity between the initial (C_o) and the equilibrium (C_e) concentration. The quantity of adsorbed U(VI) on adsorbents after the equilibrium (q_e) were measured using the equations here under:

$$q_e = \frac{(C_0 - C_e) \times V}{m} \tag{S1}$$

where C_o and C_e are the initial and equilibrium concentrations of the metal ion ($mg \cdot g^{-1}$), respectively. V is the volume of the solution (L) and m is the amount of the sorbent (g). All of the batch adsorption experiments were conducted three times, and all data in this experiment are the averages of duplicate determinations, and relative error were less than ± 5%. The corresponding to error bars were added to the experimental Figures. Effect of solution pH on the adsorption capacity was carried out with initial U(VI) concentration of 50 $mg \cdot L^{-1}$ over the pH range from 2 to 5.5 at 298 K. The intended pH of the system was adjusted by the addition of insignificant amounts of 1.0, 0.1 or 0.01 $mol \cdot L^{-1}$ HNO_3 or Na_2CO_3.

S4 Sorption kinetic

The adsorption kinetics was investigated by the adsorption data at different contact time of Fe/P-CN-800. 5.00 mg Fe/P-CN-800 was added to 50 mL of 50 $mg \cdot L^{-1}$ U(VI) solution, and stirred in a polyethylene test tubes under pH = 4.5 and T = 298 k. To assess the dependence of U(VI) adsorption on time, an aliquot of the solution was collected from 5 to 420 min after adsorption, respectively. The aliquots were centrifuged, and the supernatants were analyzed by visible spectrophotometer at 650 nm. The linear formation of pseudo-first-order kinetic model pseudo-second order kinetic and Intraparticle diffusion models were given as following Eqs. (S2-S4) [2, 3].

$$\ln(q_e - q_t) = \ln q_e - k_1 t \tag{2}$$

$$\frac{t}{q_t} = \frac{1}{k_2 q_e^2} + \frac{t}{q_e} \tag{3}$$

$$q_t = k_{int} t^{0.5} + C \tag{4}$$

where k_1 (min^{-1}), k_2 ($g \cdot mg^{-1} \cdot min^{-1}$) and k_{int} ($mg \cdot g^{-1} \cdot min^{-0.5}$) refer to the rate constants of pseudo-first-order, pseudo-second-order kinetic models, and intraparticle diffusion constant. q_e and q_t are the amounts of adsorbed U(VI) ($mg \cdot g^{-1}$) at equilibrium and given time "*t*", respectively. C ($mg \cdot g^{-1}$) is a constant proportional to the extent of boundary layer thickness. The linear plots of $\ln(q_e\text{-}q_t)$ vs. *t*, t/q_t vs. *t*, and q_t vs. $t^{0.5}$ were drawn to obtain the correlation coefficient value (R^2). The comparison of R^2 is a means of assessing the applicability of the model, and thus, elucidating the removal mechanism of the Fe/P-CN-800.

S5 Sorption isotherms

To investigate U(VI) adsorption isotherms, the U(VI) solutions with concentrations of 5, 10, 15, 20, 30, 40, 50 and 70 ppm U(VI) were prepared, and the pH of each solution was adjusted to 4.5 by adding NaOH solution. Then, 5.00 mg Fe/P-CN-800 was added to a polyethylene test tubes containing 50 mL of U(VI) solution. The mixture was thoroughly stirred for 300 min at 283, 298, and 308 K, respectively. The aliquots were centrifuged, and the supernatants were analyzed using visible spectrophotometer at 650 nm. Generally, the derivation of the Sips or Langmuir–Freundlich isotherm model, represented by Eq. (S5) assumed that at low sorbate concentrations it effectively reduces to the Freundlich isotherm and thus does not obey Henry's law; at high sorbate concentrations, it predicts a monolayer sorption capacity characteristic of the Langmuir isotherm. The Langmuir model is illustrated in the following equation (S6), which is usually used to describe the monolayer sorption process [4]. Whereas Freundlich model proposes an empirical model that is based on adsorption on heterogeneous surfaces and can be expressed as Eq. (S7) [5].

$$q_e = \frac{a_s C_e^{\beta_s}}{1 + K_s C_e^{\beta_s}} \qquad (S5)$$

$$q_e = \frac{q_m K_L C_e}{1 + K_L C_e} \qquad (S6)$$

$$q_e = K_F \times C_e^{1/n} \qquad (S7)$$

where q_e is the amount adsorbed at equilibrium (mg·g^{-1}) and C_e is the equilibrium concentration (mg·L^{-1}), q_m is the maximum adsorption amount or the saturated amount (mg·g^{-1}), a_S=q_m·K_s is the Sips model isotherm constant (L·g^{-1}), Ks the Sips model constant (L·mg^{-1}) and β_s the Sips model exponent, K_L is an equilibrium constant related

to the binding strength ($L \cdot mg^{-1}$), n and K_F are Freundlich constants which are indicators of the adsorption capacity and adsorption intensity, respectively.

The D-R isotherm, a semi-empirical equation, can provide more important information about chemical or physical properties and its linear form is given in Eq. (S8) [6].

$$\ln q_e = \ln q_{DR} - \beta\varepsilon^2 \tag{S8}$$

where q_e and q_{DR} are the sorption amount per mass of sorbent ($mol \cdot g^{-1}$) and the theoretical sorption capacity ($mol \cdot g^{-1}$), β is the constant related to the sorption energy ($mol^2 \cdot kJ^{-2}$), ε is the Polanyi potential, $\varepsilon = RT\ln(1 + 1/C_e)$, R is the gas constant ($kJ \cdot mol^{-1} K^{-1}$), and T is the absolute temperature (K).

The mean free energy of sorption is the free energy change when one mole of ions is transferred to the surface of absorbents from infinity in the solution, and its formula is Eq. (S9).

$$E_{DR} = \frac{1}{\sqrt{2\beta}} \tag{S9}$$

The magnitude of E can be related to the reaction mechanism. If E is in the range of 8-16 $kJ \cdot mol^{-1}$, the sorption is governed by chemical adsorption [7]. In the case of E < 8.0 $kJ \cdot mol^{-1}$, physical forces may affect the sorption mechanism.

S6 Thermodynamic studies

The adsorption thermodynamics parameters are analyzed by Eqs. (S10-S11) [8].

$$\ln K_d = \frac{\Delta S^o}{R} - \frac{\Delta H^o}{RT} \tag{S10}$$

$$\Delta G^o = \Delta H^o - T\Delta S^o \tag{S11}$$

where K_d is the distribution coefficient ($mL \cdot g^{-1}$) of U(VI), T is the absolute temperature (K) and R is the ideal gas constant (8.314 $J \cdot mol^{-1} \cdot K^{-1}$).

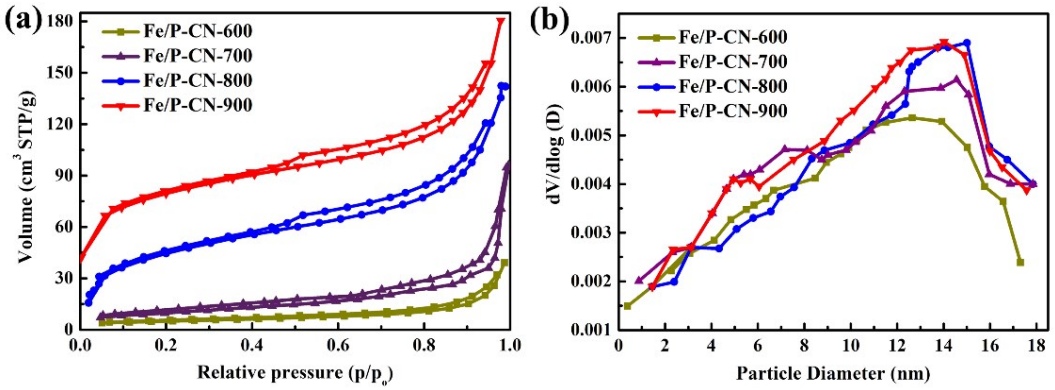

Fig. S1 (a) N_2 adsorption-desorption isotherms; (b) BJH pore size distribution of Fe/P-CN-X.

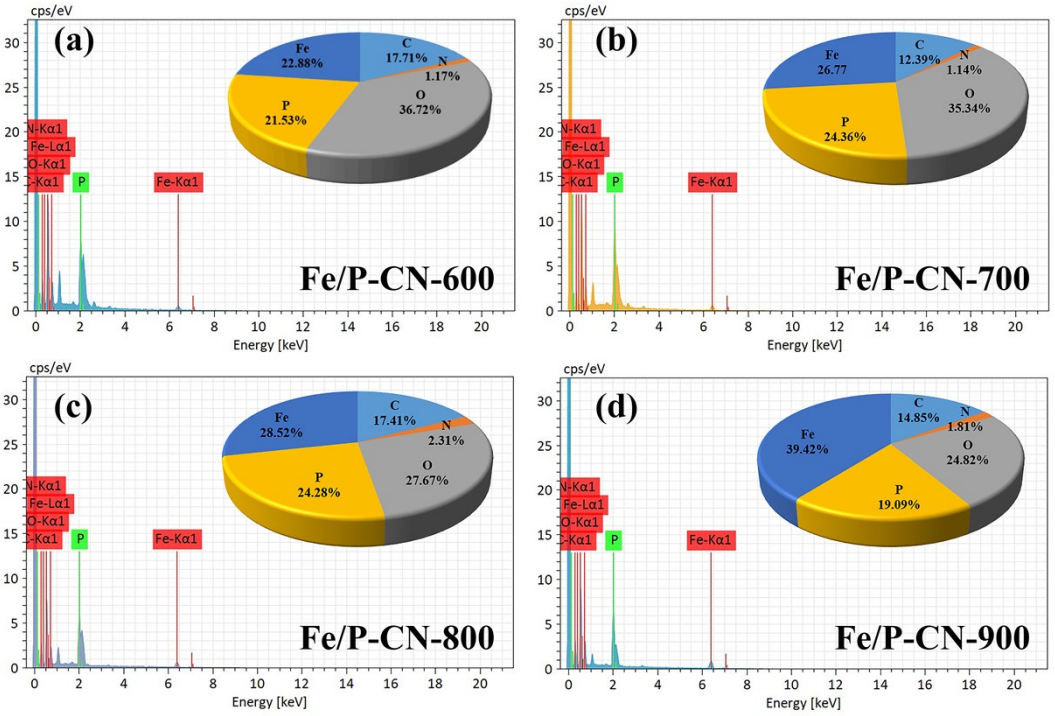

Fig. S2 EDS analysis of Fe/P-CN-X (inset: Sample surface area element composition)

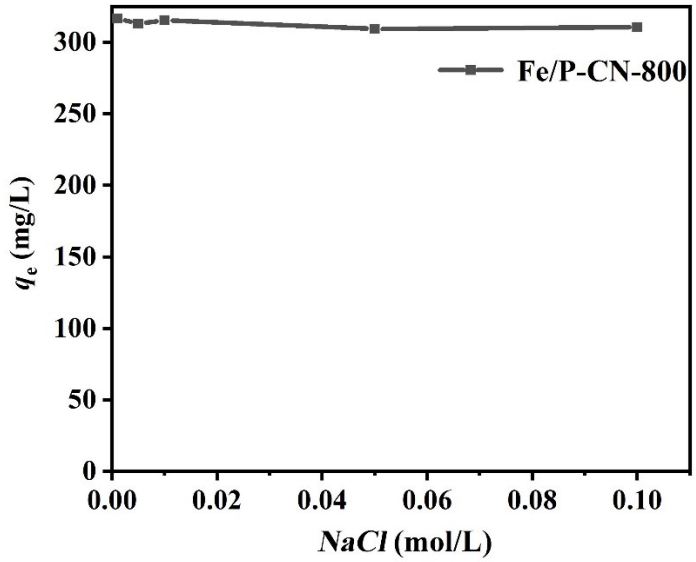

Fig. S3 Removal behaviors of U(VI) on Fe/P-CN-800 as a function of ionic strength. (m/V = 0.1 g·L^{-1}, pH = 4.5, C_0 = 50 mg·L^{-1}, T = 298.15 K and t = 300 min)

The removal behavior is not dependent on ionic strength (Fig. S2), but is primarily controlled by inner-sphere surface complexation.

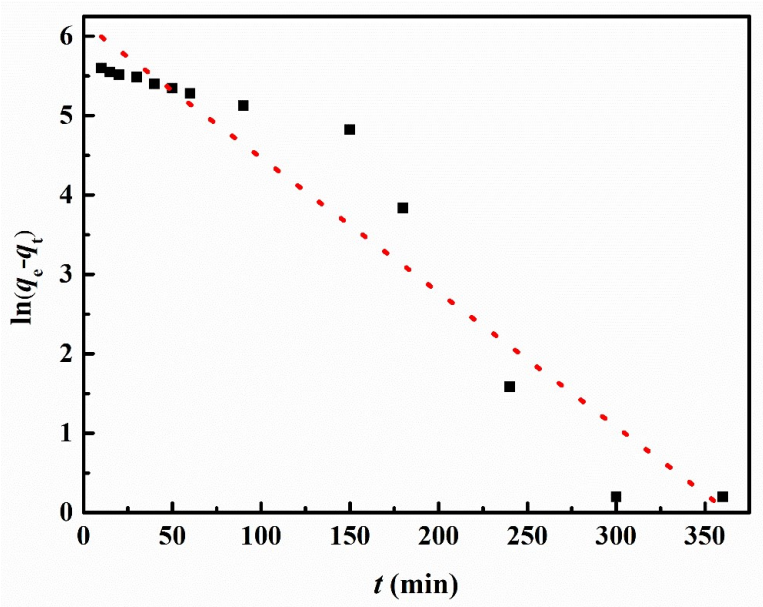

Fig. S4 The fit curve of pseudo-first-order model.

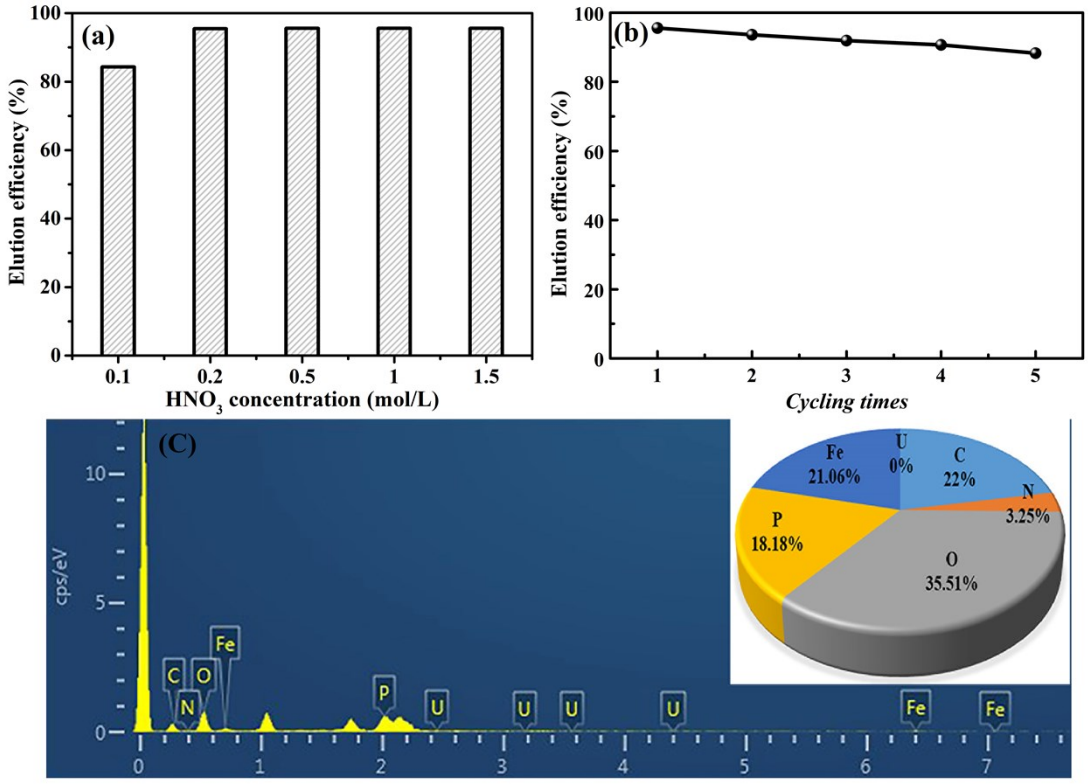

Fig. S5 (a) Elution efficiency of different concentration HNO_3 solution; (b) The removal efficiencies of U(VI) from Fe/P-CN-800 in five times repeated experiments; (c) EDS analysis of after five cycle times (inset: Sample surface area element composition).

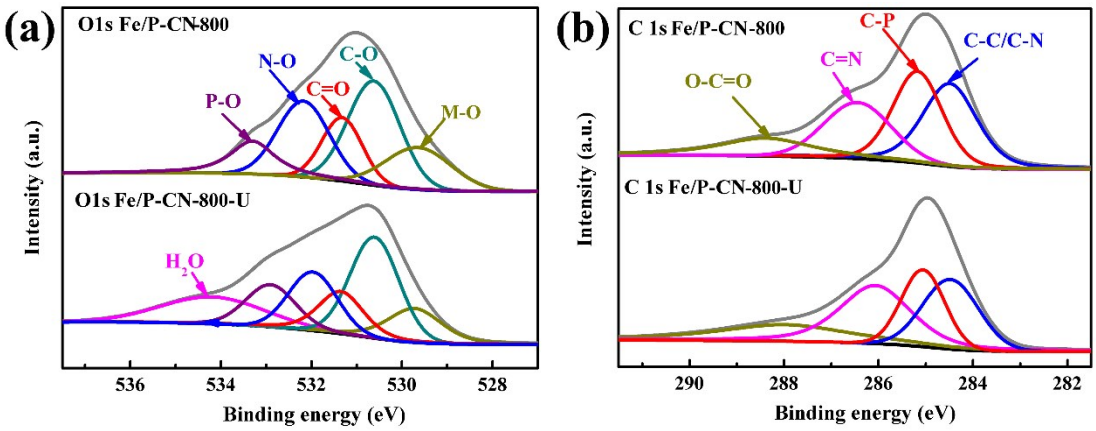

Fig. S6 XPS spectra of (a) O 1s and (b) C 1s for Fe/P-CN-800 and Fe/P-CN-800-U.

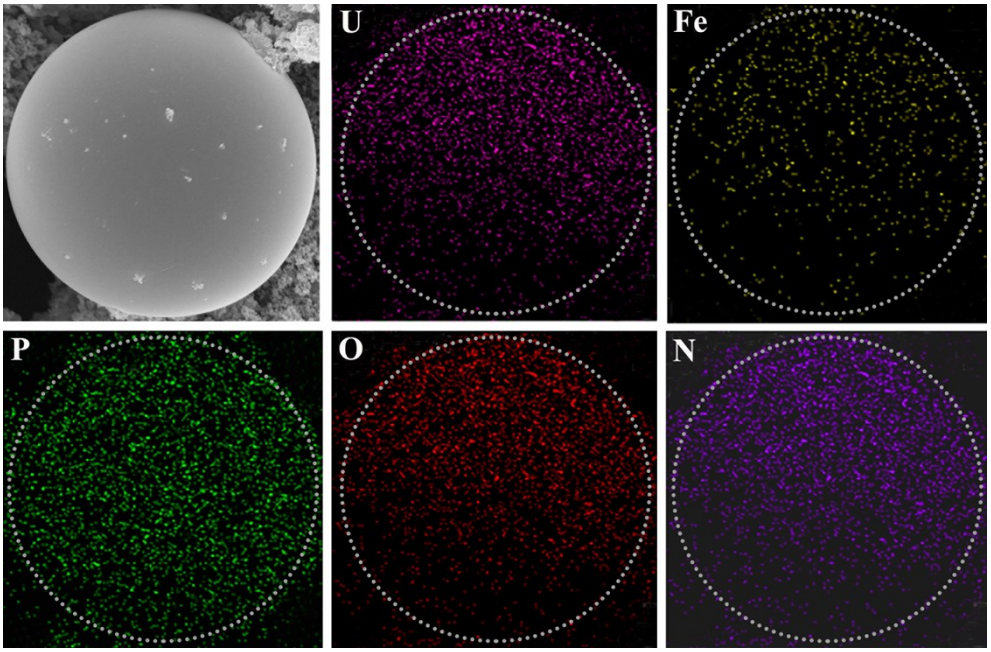

Fig. S7 SEM image and element mapping of Fe/P-CN-800-U

Table S1 S_{BET}, V_t, average pore diameters of obtained Fe/P -CN -X

absorbents	S_{BET} ($m^2 \cdot g^{-1}$)	V_t($cm^3 \cdot g^{-1}$)	D_A(nm)
Fe/P -CN -600	39.81	0.13	10.87
Fe/P -CN -700	99.32	0.19	12.87
Fe/P -CN -800	234.02	0.24	12.97
Fe/P -CN -900	334.36	0.25	13.07

Table S2 Kinetic parameters of absorbents

Sorbents	$q_{e,exp}$ ($mg \cdot g^{-1}$)	Pseudo-first-order kinetic			Pseudo-second-order kinetic			Intraparticle diffusion						
		$q_{1,cal}$ ($mg \cdot g^{-1}$)	k_1 (min^{-1})	R^2	$q_{2,cal}$ ($mg \cdot g^{-1}$)	k_2 ($g \cdot mg^{-1} \cdot min^{-1}$)	R^2	k_{int}^1	R^2	k_{int}^2	R^2	k_{int}^3	R^2
Fe/P-CN-800	309.63	298.29	1.18×10^{-2}	0.87	310.54	5.16×10^{-5}	0.99	34.03	0.99	14.49	0.99	0.39	0.79

Table S3 Isotherm parameters for adsorption of U(VI) onto Fe/P-CN-800

Isotherm models	parameters	T(K)		
		283	298	308
Sips	a_s	8.92	28.69	41.28
	K_s	0.028	0.077	0.099
	q_m	318.57	372.60	416.97
	β_s	0.95	0.97	0.99
	R^2	0.98	0.98	0.98
Langmuir	q_m	460.23	454.66	471.23
	b_L	0.035	0.090	0.114
	R^2	0.96	0.97	0.96
Freundlich	K_F	24.57	66.06	75.65
	n_F	1.36	2.02	1.81
	R^2	0.92	0.93	0.85
Dubinin-Radushkevich	q_{DR}	2.798	2.796	2.567
	β	0.0052	0.00463	0.00392
	E_{DR}	9.81	10.38	11.36
	R^2	0.97	0.95	0.97

Table S4 Thermodynamic parameters for adsorption of U(VI) onto Fe/P-CN-800

Adsorbents	ΔH^o (kJ·mol^{-1})	ΔS^o (J·mol^{-1}·K^{-1})	ΔG^o (kJ·mol^{-1})				
			283.15 K	293.15 K	303.15 K	308.15 K	313.15 K
Fe/P-CN-800	4.29	62.22	-10.52	-13.95	-14.57	-14.88	-15.19

References

[1] C. L. Zhang, Y. Liu, X. Li, H. X. Chen, T. Wen, Z. H. Jiang, Y. J. Ai, Y. B. Sun, T. Hayat and X. K. Wang, Highly uranium elimination by crab shells-derived porous graphitic carbon nitride: Batch, EXAFS and theoretical calculations, *Chem. Eng. J.*, **2018**, *346*, 406-415.

[2] D. Borah, S. Satokawa, S. Kato and T. Kojima, Sorption of As (V) from aqueous solution using acid modified carbon black, *J. Hazard Mater.*, **2009**, *162*, 1269-1277.

[3] B. Han, E. Y. Zhang, G. Cheng, L. J. Zhang, D. W. Wang and X. K. Wang, Hydrothermal carbon superstructures enriched with carboxyl groups for highly efficient uranium removal, *Chem. Eng. J.*, **2018**, *338*, 734-744.

[4] C. L. Zhang, X. Li, Z. H. Jiang, Y. H. Zhang, T. Wen, M. Fang, X. L. Tan, A. Alsaedi, T. Hayat and X. K. Wang, Selectively Immobilization of High-Valent Radionuclides by Carboxyl Functionalized Mesoporous Silica Microspheres: Batch, XPS and EXAFS Analyses, *ACS Sustainable Chem. Eng.*, **2018**, *6*, 15644-15652.

[5] F. Walton, Ion exchange, *Anal. Chem.,* **1959**, *44*, 256-70.

[6] L. L. Wang, F. Luo, L. L. Dang, J. Q. Li, X. L. Wu, S. J. Liu, M. B. Luo, Ultrafast

high-performance extraction of uranium from seawater without pretreatment using an acylamide-and carboxyl-functionalized metal-organic framework. *J. Mater. Chem. A.,* **2015**, *3*, 13724-13730.

[7] Y. Petrova, A. Pestov and L. Neudachina, Removal of metal ions in fixed bed from multicomponent solutions using N-(2-sulfoethyl) chitosan-based sorbents. *Sep. Sci. Technol*. **2016**, *51*, 1437-1445.

[8] L. Zhang, Y. Li, H. Guo, H. H. Zhang, N. Zhang, T. Hayat, Y. B. Sun, Decontamination of U(VI) on graphene oxide/Al_2O_3 composites investigated by XRD, FT-IR and XPS techniques, *Environ. Pollut*. **2019**, *248*, 332-338.